

Article

# The Effects of Additives, Particles Load and Current Density on Codeposition of SiC Particles in NiP Nanocomposite Coatings

Donya Ahmadkhaniha \* and Caterina Zanella 

Department of Materials and Manufacturing, School of Engineering, Jönköping University, P.O. Box 1026, Gjuterigatan 5, SE-551 11 Jönköping, Sweden

\* Correspondence: donya.ahmadkhaniha@ju.se

Received: 4 July 2019; Accepted: 26 August 2019; Published: 29 August 2019



**Abstract:** In this study, electrodeposition of NiP composite coatings with the addition of SiC 100 nm was carried out on low carbon steel studying the effect of additives (sodium dodecyl sulfate, saccharin), particles load (10 or 20 g/L) and current density (1, 2 and 4 A/dm<sup>2</sup>). As a benchmark, coatings from an additive-free bath were also deposited, despite additives being essential for a good quality of the coatings. The coating's morphology and composition were evaluated by scanning electron microscope (SEM) equipped with energy dispersive spectroscopy (EDS). It was shown that by addition of sodium dodecyl sulfate (SDS), pure NiP coating with a higher P content was achieved, and their morphology changed to nodular. SDS also reduced the codeposited fraction of SiC particles, while saccharin increased it. SiC loading and current density had less impact respect to the additives on codeposition of SiC particles. Finally, the microhardness of NiP coatings did not increase linearly by codeposition of SiC particles.

**Keywords:** NiP coating; composite coating; additives; SiC particle; microhardness

## 1. Introduction

Nickel-based alloy coatings and composites have been studied as substitutes for hard chromium coating, in which the production is currently restricted by Registration, Evaluation, Authorisation and Restriction of Chemicals (REACH) regulations [1]. NiB and NiP coatings are two alternative coatings due to their properties. NiB coatings have high hardness, wear and abrasion resistance but are limited to applications within microelectronic industries and have much higher running costs. In contrast, NiP coatings have a more comprehensive industrial application due to their high corrosion resistance [2–11]. NiP coatings can be categorized into three groups according to phosphorous content: Low phosphorous, from 2 wt.% to 5 wt.%; medium phosphorous, from 6 wt.% to 9 wt.%; and high phosphorous, between 10 wt.% and 13 wt.%. By increasing the P content of the coatings, corrosion resistance improves while the hardness and wear resistance of the coatings decrease [3,7]. Although NiP coatings have been deposited mainly by the electroless technique, electrodeposited NiP coatings are a relatively new research topic and have attracted attention in recent years due to their low cost, easy manufacturability and rapidity [11].

The hardness of NiP coatings is not sufficiently high for some demanding applications, although there is a possibility of further hardening by heat treatment of NiP coatings when the substrate is able to withstand the heat treatment. In order to harden the coating without heat treatment, the coatings can be reinforced with hard particles, which has demonstrated high hardness and proper wear resistance compared to pure metal or alloy coatings [12–16]. The properties of composite coatings depend primarily on the matrix, the amount and the distribution of co-deposited particles.

Meanwhile, the amount and distribution of particles are related to electrodeposition parameters including particle characteristics (particle shape, size, concentration and surface charge), electrolyte composition (additives, surfactant type and concentration), pH and applied current (direct or pulsed current and current density) [17–21]. Several studies have reported the effect of process parameters on the amount of codeposited particles in the metal matrix [18–25]. However, a low number of particles are usually codeposited in the case of nanoparticles, and they tend to agglomerate, which results in the poor mechanical behaviour of the coatings. Hence, increasing the amount of codeposition as well as improving the particle distribution in the matrix are the crucial issues that require further investigation.

It is well known that introducing additives to the electrolyte affects the properties and appearance of deposits [20,22,25]. Additives can be categorised based on their application as grain refiners, levelling agents, and wetting agents or surfactants. Saccharin is a common brightening agent in the electrodeposition of nickel, which refines grains, inhibits the hydrogen evolution reaction and reduces the internal stress of the coatings [25–28]. In previous studies, it was shown that the addition of saccharin significantly improves the cathode current efficiency of the NiP electrodeposition [29]. However, saccharin decreased the SiC codeposition and phosphorus content, compared to deposits obtained from saccharin-free baths [30].

Surfactants such as sodium dodecyl sulfate (SDS) are needed in the case of electrodeposition processes where the current efficiency is below 100%. Hydrogen evolution is the common secondary cathodic reaction, and SDS can reduce the residence time of the H<sub>2</sub> bubble on the cathodic surface, and also pitting as well as porosity. Surfactants are beneficial for enhancing the stability and uniformity of the electrolyte by increasing the wettability and changing the surface charge of the particles [31]. The effect of surfactants such as SDS and cetyltrimethylammonium bromide (CTAB) on the electrodeposition of composite coatings has been studied, and improvement in the distribution of SiC particles in the composite coating was shown [32–34]. Hongmin et al. [35] reported that the dispersion of 40 nm SiC in Ni–SiC coating is superior with the addition of SDS to the electrolyte as opposed to the addition of CTAB to the electrolyte. Hou et al. [36] found that the addition of CTAB decreased the agglomeration of inherently hydrophobic SiC particles in the electrolyte. Besides, the co-deposition of sub-micron SiC particles content increased with increasing concentration of CTAB in the electrolyte. Malfatti et al. [20] concluded that the addition of anionic (SDS) and cationic (cetyltrimethylammonium hydrogensulfate, CTABS) surfactants decreased the amount of co-deposited 600 nm SiC particles, indicating that the particle incorporation was practically independent of the surfactant's charge. Rundik et al. [34] found the presence of CTAB on the particles reduced the current efficiency due to a decrease in the number of metal ions adsorbed on the particles. On the other hand, the fine-grained nickel matrix of the composite with high microhardness was obtained.

Apart from additives, current density and particle loading have their impacts on the incorporation of particles, and there is a threshold for current density and particle loading above which that particle codeposition reduces [16,36,37]. Proper co-depositing of reinforcing particles within the NiP matrix can produce a coating with improved hardness, corrosion and wear resistance. However, Hou et al. [36] reported that the addition of SiC particles increases the surface roughness of pure NiP coatings. This paper focuses on the comparison of the SiC codeposition in the presence of different additives, commonly used in industrial processes, under different deposition parameters. Therefore, NiP/SiC coatings were deposited on steel at different current densities and SiC loadings. Additives were added to the bath to find the optimized condition which can enhance the codeposition rate of nano SiC particles while maintaining the good quality of NiP matrix with low surface roughness.

## 2. Materials and Methods

Nickel high phosphorous (NiP) alloys were electrodeposited by direct plating from a modified Watts bath on low carbon steel sheets. The NiP bath was prepared according to Table 1 with additives. In order to study the effect of additives, three different baths, as listed in Table 1, were prepared. Bath 1 was additive-free, bath 2 had 3 g/L of saccharin, and bath 3 contained both saccharin and

SDS. The deposition was carried out in a thermostated cell with a wall thickness of 2 cm, and a bath volume of 2 L. The distance between the vertical anode (Ni sheet with a purity of 99.9%) and cathode was 12 cm. The pH of the solution was adjusted by adding sulfuric acid or sodium hydroxide and kept constant (pH: 2.15) with continuous adjustment. Either 10 or 20 g/L of silicon carbide ( $\beta$ -SiC, provided by GetNanoMaterials, Saint-Cannat, France) particles with the average size of 100 nm were added and dispersed by magnetic stirring for 24 h before plating. During electroplating, stirring was maintained at 250 rpm with a magnetic stirrer (6 cm width and 0.7 cm diameter) to produce the composite coatings. The size of the SiC particles was chosen according to previous results [7]. Composite coatings were named according to the SiC loading in the bath as NiP/10SiC and NiP/20SiC in this study. Electrodeposition was carried out at 70 °C with 1, 2 and 4 A/dm<sup>2</sup> current densities.

**Table 1.** Deposition baths and parameters.

Chemical Compositions	g/L	Bath 1	Bath 2	Bath 3	Parameters
NiSO <sub>4</sub> ·7H <sub>2</sub> O	100–150	✓	✓	✓	<i>i</i> : 1, 2, 4 A/dm <sup>2</sup>
NiCl <sub>2</sub> ·6H <sub>2</sub> O	15–30	✓	✓	✓	<i>T</i> : 70 °C
H <sub>3</sub> BO <sub>3</sub>	15–30	✓	✓	✓	Agitation: 250 rpm
H <sub>3</sub> PO <sub>3</sub>	100–130	✓	✓	✓	Anode: Pure Ni sheet
SiC	10, 20	✓	✓	✓	pH: 2.15
Sodium dodecyl sulfate	0–1	–	–	✓	–
Saccharin	0–3	–	✓	✓	–

Before electrodeposition, the steel substrates were pre-treated by mechanically grinding with SiC paper (abrasive paper, grades #500 and #800) to remove the surface oxide layer, cleaned ultrasonically in an alkaline soap and activated by pickling for 8 min in 2.5 M H<sub>2</sub>SO<sub>4</sub> at 50 °C. The current efficiency was evaluated by measuring the weight of the coating and comparing with the theoretical deposited mass. The weight of the coating ( $\Delta m$ ) was determined by weighing the substrate before and after plating with high precisions scales ( $\pm 0.0001$ ). The Faraday law (Equation (1)) was used to calculate the theoretical mass ( $m_t$ ) of the coating during deposition, and finally, current efficiency was calculated according to Equation (2).

$$m_t = \left( x_1 \frac{M_1}{N_1} + x_2 \frac{M_2}{N_2} \right) \times \frac{I_t}{F} \quad (1)$$

$$\text{Current efficiency (CE)\%} = \frac{\Delta m}{m_t} \times 100 \quad (2)$$

where,  $M_1$  and  $M_2$  are the molar mass of the Ni and P, respectively.  $N_1$  and  $N_2$  are the electrons exchanged during deposition by the Ni and P;  $x_1$  and  $x_2$  are the molar fraction of Ni and P, respectively; in the final coating,  $I$  is the applied current (A),  $t$  is the total time of deposition (s), and  $F$  is the Faraday's constant (96,485 coulombs).

The deposition was carried out for 1 h, and the coating thickness varied between 20 to 35  $\mu$ m depending on the current efficiency.

After deposition, the surface of the coatings was studied by scanning electron microscopy (SEM, JSM-7001F, JEOL, Akishima, Japan) equipped with energy dispersive spectroscopy (EDS, 55100, EDAX, Mahwah, NJ, USA) to characterize both the morphology and composition of the coatings. SEM and EDS analyses were run at 15 kV, and probe current of 14 A. SEM images were captured by secondary electrons. The spectrum of five different areas on each sample was collected, and then the average composition of the coatings and their standard deviation were calculated. The microhardness of the coatings was measured on the coating's cross-section (centerline of the cross-section) by a Vickers indenter (NanoTest<sup>TM</sup> Vantage, 40.36, Micro Materials, Wrexham, UK) with an indentation load of 200 mN and dwell time of 10 s. Fifteen measurements were run for each coating, and their average and standard deviation were calculated.

### 3. Results and Discussions

#### 3.1. Deposition Current Efficiency (CE)

Figure 1 shows the current efficiency (CE) of the deposition in different conditions. As seen, the current efficiency in baths 1 and 2 changed between 40% to 70% (considering the error bars) depending on the SiC loading and current density. In the additive-free bath (bath 1), increasing current density enhanced the CE of pure NiP, while adding either SDS (bath 3) or saccharin (bath 2), the highest CE was achieved at 1 A/dm<sup>2</sup> for pure NiP coatings. In the case of the composite bath regardless of the SiC loading, maximum CE was achieved mainly at 1 or 2 A/dm<sup>2</sup>. Higher current density increased the H<sub>2</sub> evolution and therefore reduced the CE. It has also been reported that SiC particles can adsorb protons and consequently, result in increased hydrogen evolution [29,38,39]. In this study, CE varies in a wide interval, and neither addition of SiC nor increasing current density decreased the CE values. Nor did CE increase with the addition of saccharin. Hence, the contribution of these different parameters demonstrates a complicated process which does not show a trend.

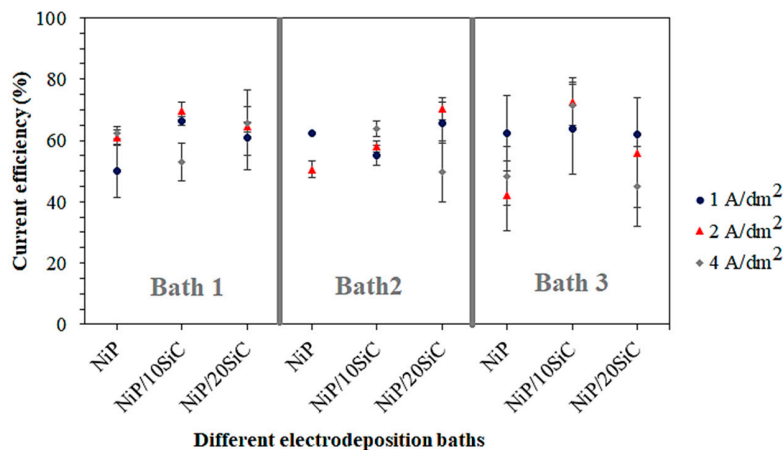
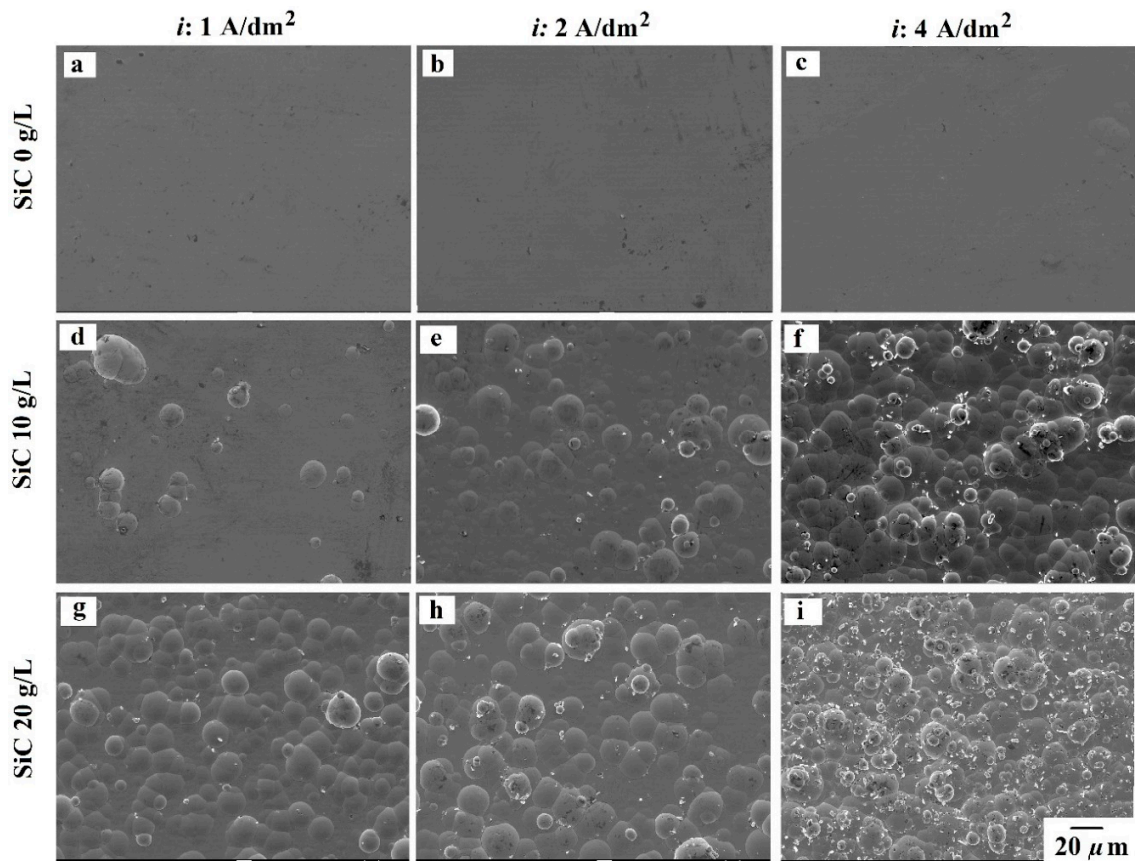


**Figure 1.** Effect of SiC loading, SDS, saccharin as well as current density on current efficiency of electrodeposition NiP coating.

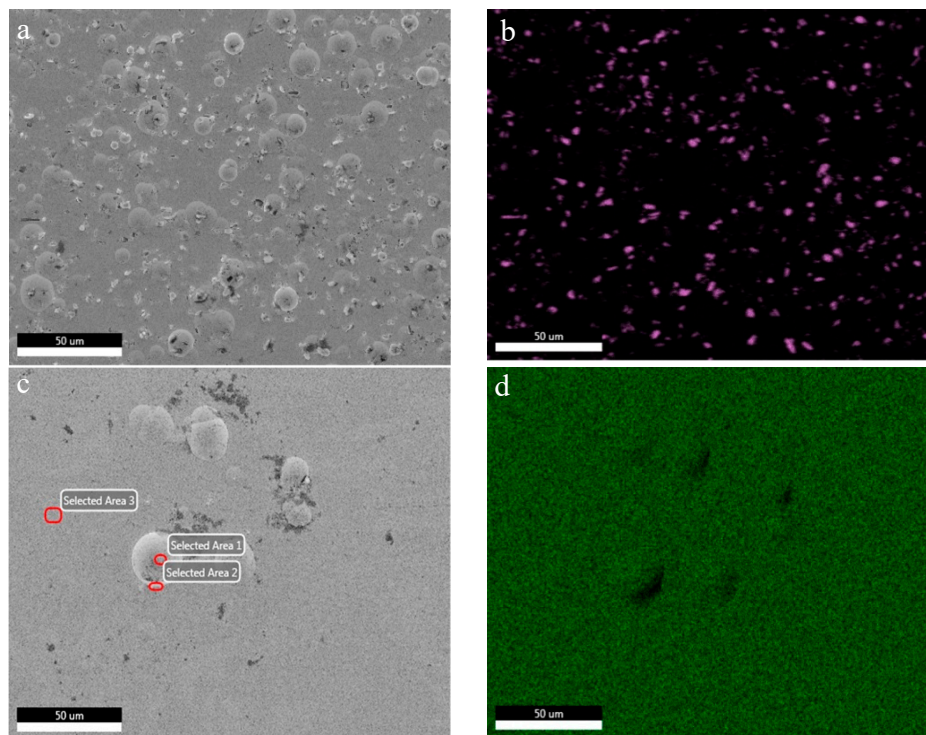
#### 3.2. Coatings Morphology

Figure 2 exhibits the surface morphology of the coatings obtained at different conditions. NiP coatings (Figure 2a–c) deposited from bath 1 have a smooth surface without any features, and even by increasing the current density, their morphology did not change. Whereas, the addition of SiC particles in the bath results in nodular morphology (Figure 2d–f) and by increasing the SiC loading (Figure 2g–i) as well as current density, the nodularity increased. It seems that by increasing both current density and SiC particles, more nucleation sites can be produced which reduces the size of those domains and resulting in finer nodules. The nodular morphology was observed by other researchers as well [40–42]. Sarret et al. [40] found similar nodular morphology of NiP coating with the addition of nano-sized SiC particles, although NiP coatings were deposited from a different bath from that which was used in this study. Mafi et al. [41] deposited electroless NiP coatings with nodular morphology; they also observed that surfactant concentration affects the morphology of the coatings while in the presence of SDS, nodular morphology of NiP/Polytetrafluoroethylene (PTFE) coatings was achieved at all studied concentrations of SDS. The small white areas on the surface of the coatings (Figure 3a) are SiC particles as confirmed by EDS map in Figure 3b, and it can be seen that SiC particles were agglomerated. Figure 3d demonstrated the EDS map of P on NiP/20SiC coatings. It can be seen in Table 2, that the nodules (area 1) have the same wt.% P (around 14%) as the flat areas (area 3) while the nodule boundary (area 2) has less wt.% P (8%).

By comparing Figure 2d–i, it is shown that by increasing the particle loading and current density, the SiC codeposition is also enhanced.



**Figure 2.** SEM images of surface of (a–c) NiP, (d–f) NiP/10SiC, (g–i) NiP/20SiC. (a,d,g)  $i$ : 1 A/dm<sup>2</sup>, (b,e,h)  $i$ : 2 A/dm<sup>2</sup>, (c,f,i)  $i$ : 4 A/dm<sup>2</sup> deposited from bath 1.



**Figure 3.** (a) SEM and (b) EDS map of Si for NiP/10SiC coating deposited from bath 2 at 1 A/dm<sup>2</sup>; (c) SEM image and (d) EDS map of P of NiP/20SiC deposited from bath 3 at  $i$ : 1 A/dm<sup>2</sup>.

Pure NiP coatings (Figure 4a–c) deposited from bath 2 (only saccharin addition) have a smooth surface, similar to the ones deposited from bath 1 (additive-free). While at 4 A/dm<sup>2</sup> (Figure 4c), some nodules were observed. In the case of composite coatings (Figure 4d–f), nodularity is evident, and the size of nodules decreased; while their population, as well as SiC particles codeposition increased by increasing SiC loading (Figure 4g–i) and current density, similar to what was observed in Figure 2. By comparing Figures 2 and 4, it seems that saccharin increased the SiC codeposition and reduced the nodular size.

**Table 2.** wt.% P of NiP/20 SiC coating, on the nodule surface and nodule boundary.

Areas	Area 1	Area 2	Area 3
wt.% P	14.35	8.02	14.28

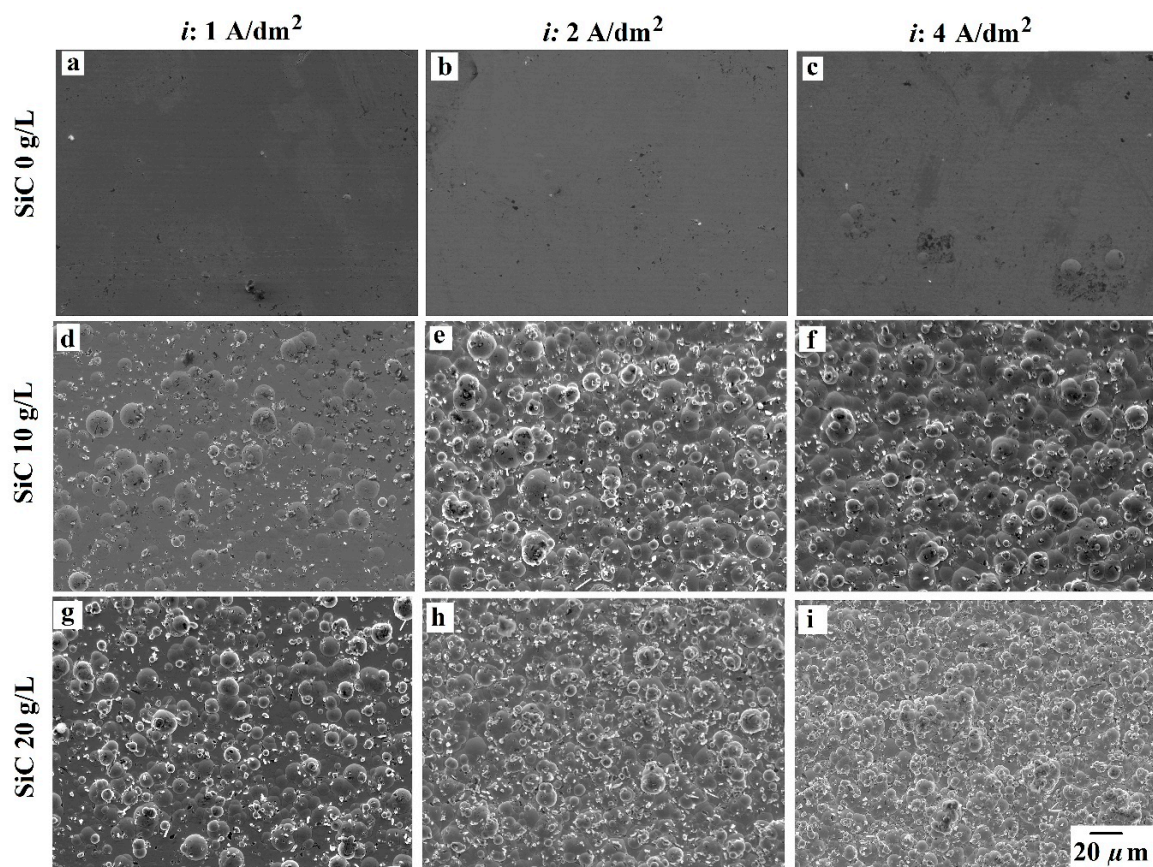


**Figure 4.** SEM images of the surface of (a–c) NiP, (d–f) NiP/10SiC, (g–i) NiP/20SiC. (a,d,g)  $i$ : 1 A/dm<sup>2</sup>, (b,e,h)  $i$ : 2 A/dm<sup>2</sup>, (c,f,i)  $i$ : 4 A/dm<sup>2</sup> deposited from bath 2.

In the presence of both SDS and saccharin (bath 3), nodularity appeared even in pure NiP coating at current densities of 2 and 4 A/dm<sup>2</sup> (Figure 5b,c). Less SiC particles are seen on the surface of composite coatings. The morphology of the composite coatings in Figure 5 is similar to the ones in Figure 2 at current densities of 1 and 2 A/dm<sup>2</sup>.

These results showed that higher current density and addition of SiC particles changed the morphology of the coatings to nodular. On the other hand, SDS addition reduced the SiC incorporation, while increasing nodularity.

This nodular morphology has been observed by Grosjean et al. [43] where micron-sized SiC particles are incorporated into a NiP matrix, but also in NiP deposition without particles [3,44]. Grosjean et al. [43] related the nodular morphology to the formation of phosphorus, while Kalantray et al. [44] attributed it to an increase of the bath pH since by increasing the pH the phosphorus content of the

deposit reduces and the number of nodules on the surface increases. Sarret et al. [40] believed that the formation of these nodules is not due to a reduction of the phosphorous content but related to a change in the growth mechanism promoted by the incorporation of the nanoparticles. The codeposition of particles to the NiP matrix modify the surface finish in terms of brightness and surface roughness. The NiP coatings obtained in this study are bright and smooth, while after the addition of SiC particles, the surface becomes matt and rougher, depending on the codeposition percentage. Amell et al. [45] attributed the formation of nodules to the weight fraction of nanoparticles in the coating. In this study, pH was adjusted before plating. However, the local pH can increase due to the H<sub>2</sub> evolution during the deposition. The EDS map, also in Figure 3d, confirms that some nodules boundaries have less P content than the other areas. As a result, the formation of the nodule can be attributed to a local increase in pH by increasing current density and changing growth mechanism by adding nano SiC particles.

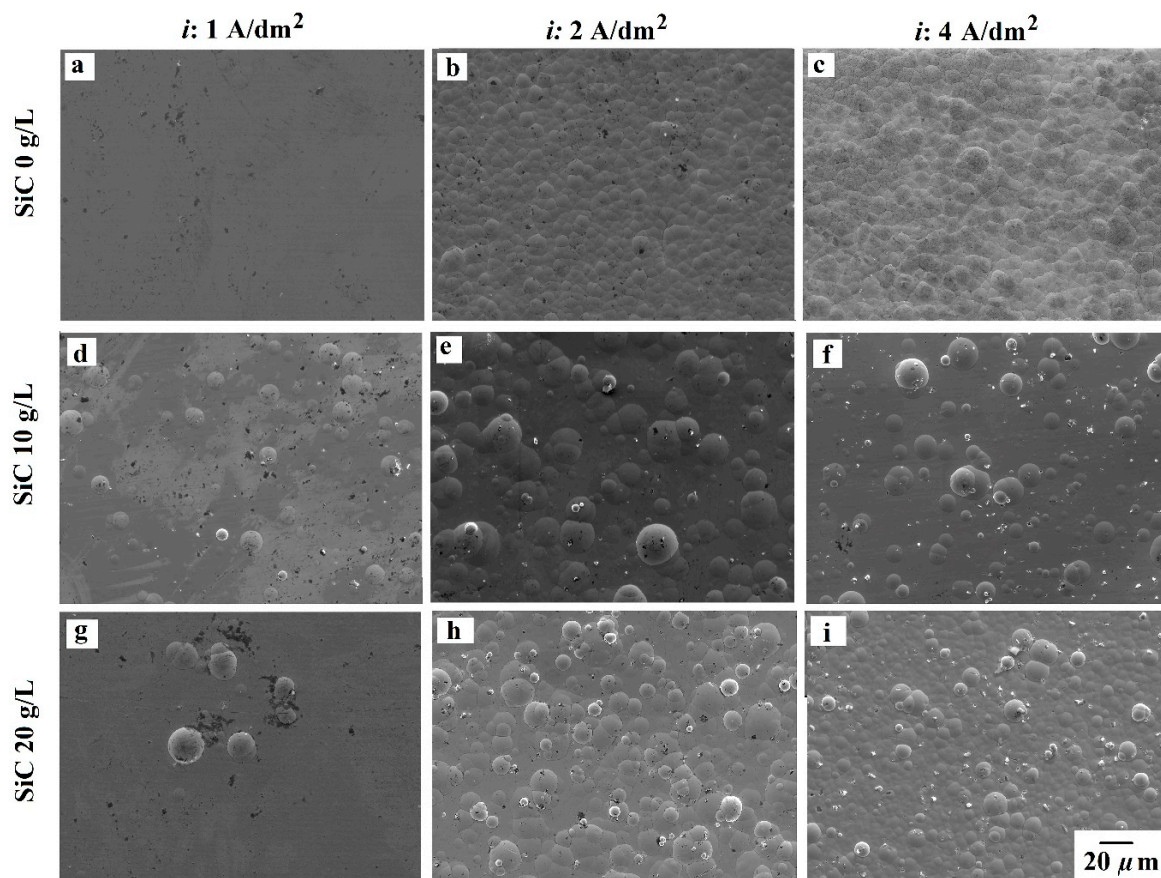


**Figure 5.** SEM images of the surface of (a–c) NiP, (d–f) NiP/10SiC, (g–i) NiP/20SiC. (a,d,g)  $i$ : 1 A/dm<sup>2</sup>, (b,e,h)  $i$ : 2 A/dm<sup>2</sup>, (c,f,i)  $i$ : 4 A/dm<sup>2</sup> deposited from bath 3.

### 3.3. Coatings Composition

Coatings composition was analysed by EDS on the surface of the coatings, and the results are plotted in Figure 6. According to Figure 6a, all coatings have more than 10 wt.% P which confirms the deposition of Ni high P coating. Pure NiP coating has a bit higher P content than composite coatings. Lower wt.% P was obtained by increasing SiC loading in deposited coatings from bath 2. Moreover, increasing current density decreased wt.% P for coating produced in baths 1 and 2. The composition of the coatings produced from bath 3 does not obey the same rule as the others and the wt.% P of pure NiP coating from bath 3 is higher than the pure coatings obtained from baths 1 and 2.

The wt.% SiC particles in the coatings are shown in Figure 6b. Maximum wt.% SiC was achieved from bath 2, and by increasing the current density, more SiC particles were codeposited in bath 2. Meanwhile, the dispersion of wt.% SiC became less uniform by increasing current density since higher

error bars can be seen at 2 and 4 A/dm<sup>2</sup> respective to 1 A/dm<sup>2</sup>. According to Figure 6b, saccharin has the most impact on codeposition of SiC particles, and SDS decreases SiC particles incorporation. Figure 6c shows only a slight trend between wt.% P and codeposition of SiC particles in the NiP matrix, but some other factors might affect the wt.% P in the matrix.

The increase in wt.% SiC particles in bath 1 by increasing current density to 4 A/dm<sup>2</sup> can be attributed to the increasing tendency for adsorbed particles to arrive at the cathode surface, which is in agreement with the Guglielmi model. However, the increase in wt.% SiC by increasing current density is not observed in other conditions. The inconsistency of particle codeposition was also observed by Ünal et al. [23]. This inconsistency can also be explained by considering that the amount of codeposited particles is governed by the particle flux to the metal surface, which depends on current density according to Equation (3) [46].

$$J_p = \frac{3V_{m,M}}{4\pi r^3 z F N_A} \frac{x_v}{1 - x_v} i \quad (3)$$

where  $V_{m,M}$  is the molar volume of the metal,  $r$  is the radius of the particles,  $z$  is the charge of the metal ion,  $F$  is Faraday's constant,  $N_A$  and  $i$  are Avogadro's constant and current density, respectively, and  $x_v$  is the volume fraction of the particles in the coating. At high current densities, nickel ions are transported faster than SiC particles, which results in a lower wt.% SiC. The occurrence of hydrogen evolution also increased by increasing current density, which can hinder the codeposition of SiC particles to the matrix. There is not a clear trend for the codeposition of SiC particles with current density in bath 2 and the coatings produced in bath 3, current density did not affect the codeposition rate. It seems that the addition of these additives changed the surface states of SiC particles. SiC particles are inert while physical adsorption of ions or surfactant molecules from the electrolyte modifies the particle's surface which tends to be surrounded by an ionic cloud and promotes electrophoretic migration of the particles towards the cathode. SDS is an anionic additive that can increase the negative surface charge of particles [46] and reduce the particle's incorporation. Nevertheless, Rezaei et al. [22] observed in their study that the particles' surface charge is not the dominant factor for codeposition.

According to Figure 6b, increasing the SiC loading did not increase the codeposition of SiC particles at all current densities and wt.% SiC varied more in 20 g/L SiC loading. Increasing particle concentration in the electrolyte can increase the incorporation of SiC particles by increasing the number of SiC particles that reach the cathode. Meanwhile, higher SiC particles concentration may lead to their agglomeration due to their poor wettability, which ends up lowering SiC incorporation as seen by Walsh et al. [25]. It should be noticed that SiC particles that touched the cathode surface for a sufficient period can be successfully entrapped by growing the Ni matrix around it [16]. Hence, if higher SiC loading caused agglomeration, their entrapment adhesion in the matrix is lower, and they can be removed by the flow of the bath as seen by Ger et al. [47]. Therefore, not only SiC loading but also capturing capacity of the NiP layer determines wt.% SiC in NiP matrix. Hou et al. [36] also observed that a high concentration of SiC particles shielded the cathode surface from the flux of incoming SiC particles. It should also be considered that the same value of codeposited SiC particles (in bath 3), despite twice SiC loading in the bath, can be due to the less concentrated ratio of surfactant to SiC in NiP/20SiC than in NiP/10SiC bath.

According to the above results, it can be seen that 10 g/L SiC loading, the addition of Saccharin and current density of 1 A/dm<sup>2</sup> are the optimum conditions for deposition NiP/SiC coatings. Higher SiC loading results in SiC agglomeration, thus reducing their codeposition. SDS reduced the SiC codeposition, which can be due to the increase in the negative charge of the particles. Saccharin produced the finer nodular with more boundaries which can enhance the mechanical entrapment of SiC particles and hence increase their codeposition in the matrix.

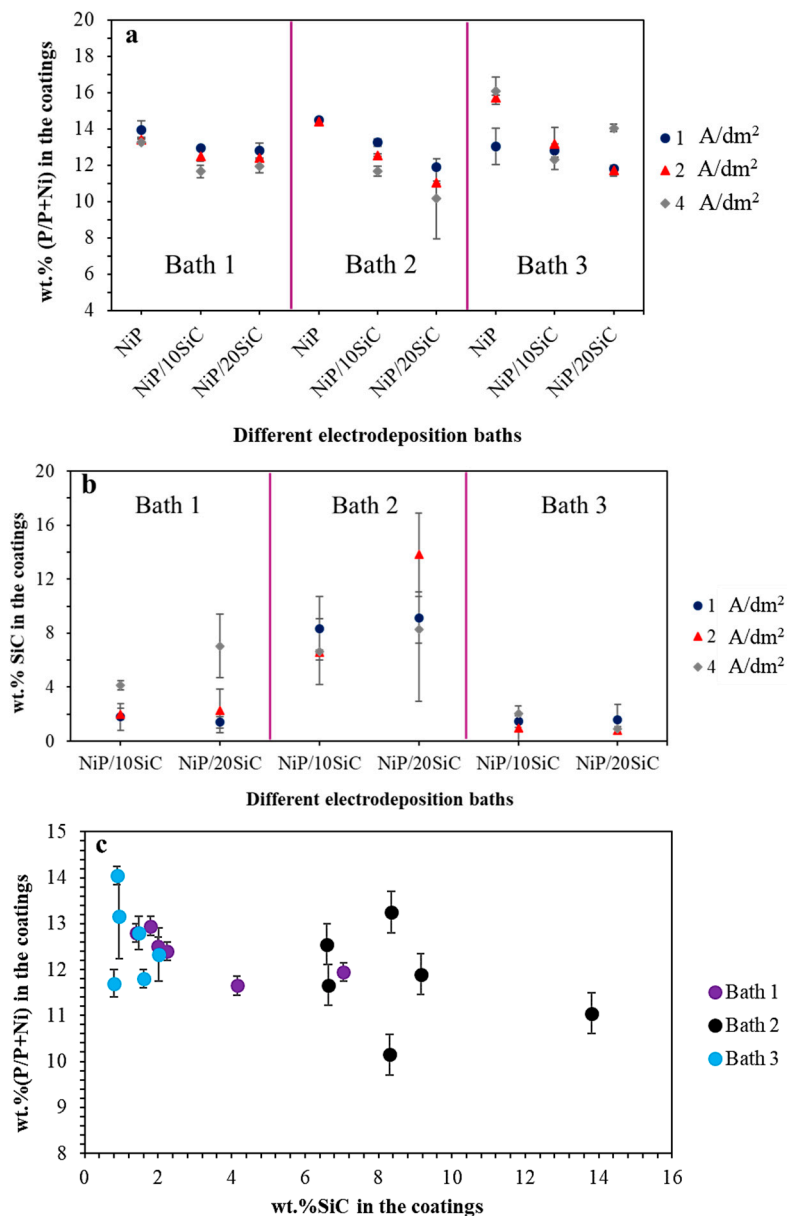


**Figure 6.** The composition of NiP and composite coatings deposited at different conditions (a) wt.% P in the metallic coating, (b) wt.% SiC (c) The relation between wt.% P and wt.% SiC in the coatings.

### 3.4. Coatings Microhardness

Microhardness of the coatings was measured on their cross-section by Vickers indenter, and the results are shown in Figure 7. Coatings deposited from bath 1 have microhardness values around 800 HV<sub>0.02</sub>, and neither increasing current density nor increasing SiC loading affect their microhardness values. A slight increase of hardness can be achieved by SiC addition in bath 2 (with saccharin), but the hardening is quite limited despite the high wt.% of SiC. Maximum microhardness (900 HV<sub>0.02</sub>) was achieved in NiP/20SiC coating deposited from bath 2 at 2, and 4 A/dm<sup>2</sup>. All the coatings deposited from bath 3 have lower microhardness values (about 750 HV<sub>0.02</sub>) than the others, even in the pure condition.

Moreover, presence of SiC particles and saccharin can change the residual stress of NiP coatings as seen by Alexis et al. [48] and Berkh et al. [30] which can influence the microhardness of the coatings as well. Alexis et al. [48] showed that the tensile stress of the coating decreases with the increase in SiC content in the electrolyte and Berkh et al. [30] exhibited that deposits with compressive stresses can be formed with increasing particle size and concentration. They also reported that by adding saccharin,

internal stresses were close to zero throughout the investigated pH range. It must be considered that not only the weight percentage of the particles but also their dispersion as well as their interface coherency with the matrix, have crucial roles in their impact on the hardness values.

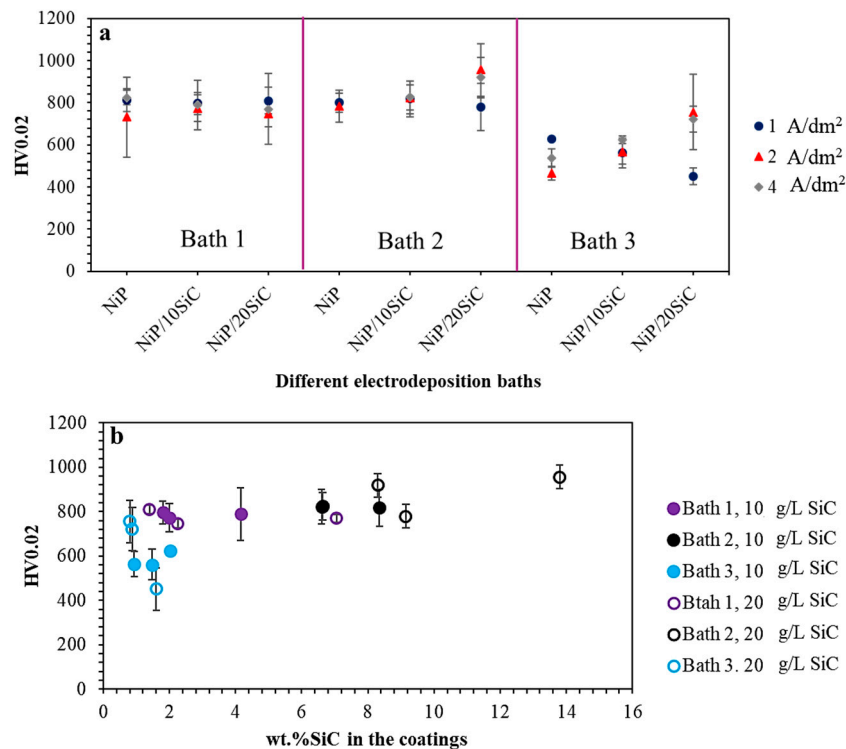


**Figure 7.** (a) Microhardness values of the coatings at different conditions; (b) the relation between microhardness and wt.% SiC.

#### 4. Conclusions

This paper focused on the codeposition of SiC nanoparticles in NiP coatings produced by electrodeposition. Due to the typical application of additives during the industrial production of such coatings, the work compared the codeposition in the presence or absence of saccharin and SDS under different process parameters. In particular, the effect of current density, SiC loading in the presence of the different additives on the codeposition of SiC particles were studied, and the following results were obtained:

- Additive-free bath produces smooth surfaces due to the amorphous state of the NiP alloys. However, the presence of the 100 nm SiC powder induced a nodular morphology. Higher current density, as well as SiC loading, resulted in more and finer nodular morphology. Regarding the additives, the addition of SDS promoted the formation of the nodules in the pure NiP coatings and promoted coarser nodules in other cases.
- The particles slightly influenced the current efficiency of the process, and therefore, pH changed a bit (From 2.15 to 2.32) during the deposition which led to a slight reduction in wt.% P of the coatings by increasing SiC particles codeposition. Additives did not influence the current efficiency noticeably, while SDS increased the P content of pure NiP coatings.
- The addition of saccharin increased the SiC codeposited fraction from 7 wt.% (maximum content of SiC in the coatings without additives) to the maximum 13 wt.%, while SDS, reduced it to 1 wt.%. There is no direct relation between codeposited wt.% SiC and the coating's microhardness values since SiC codeposition rate is not the only factor determining the hardness of these coatings, as the particles might interact with the microstructure as well.

**Author Contributions:** Conceptualisation: D.A. and C.Z.; Methodology: D.A. and C.Z.; Validation: D.A. and C.Z.; Formal Analysis: D.A. and C.Z.; Investigation: D.A. and C.Z.; Resources: D.A. and C.Z.; Data Curation: D.A. and C.Z.; Writing—Original Draft Preparation: D.A.; Writing—Review and Editing: D.A. and C.Z.; Visualisations: D.A.; Supervision: C.Z.; Project Administration: D.A. and C.Z.; Funding Acquisition: C.Z.

**Funding:** This research was funded by Horizon 2020, grant number 686135.

**Acknowledgments:** The experimental support regarding to the bath recipe of the present work by Luca Magagnin from University of Politecnico di Milano is highly acknowledged.

**Conflicts of Interest:** The authors declare no conflict of interest.

## References

1. Lekka, M.; Offoiach, R.; Lanzutti, A.; Mughal, M.Z.; Sebastiani, M.; Bemporad, E.; Fedrizzi, L. Ni-B electrodeposits with low B content: Effect of DMAB concentration on the internal stresses and the electrochemical behavior. *Surf. Coat. Technol.* **2018**, *344*, 190–196. [[CrossRef](#)]
2. Bonin, L.; Vitry, V.; Delaunois, F. Corrosion behaviour of electroless high boron-mid phosphorous nickel duplex coatings in the as-plated and heat-treated states in NaCl, H<sub>2</sub>SO<sub>4</sub>, NaOH and Na<sub>2</sub>SO<sub>4</sub> media. *Mater. Chem. Phys.* **2018**, *208*, 77–84. [[CrossRef](#)]
3. Vitry, V.; Sens, A.; Kanta, A.F.; Delaunois, F. Wear and corrosion resistance of heat treated and as-plated Duplex NiP/NiB coatings on 2024 aluminum alloys. *Surf. Coat. Technol.* **2012**, *206*, 3421–3427. [[CrossRef](#)]
4. Vitry, V.; Bonin, L.; Malet, L. Chemical, morphological and structural characterisation of electroless duplex NiP/NiB coatings on steel. *Surf. Eng.* **2017**, *36*, 475–484. [[CrossRef](#)]
5. Shakoor, R.A.; Kahraman, R.; Waware, U.; Wang, Y.; Gao, W. Properties of electrodeposited Ni–B–Al<sub>2</sub>O<sub>3</sub> composite coatings. *Mater. Des.* **2014**, *64*, 127–135. [[CrossRef](#)]
6. Vitry, V.; Sens, A.; Delaunois, F. Comparison of various electroless nickel coatings on steel: Structure, hardness and abrasion resistance. *Mater. Sci.* **2014**, *786*, 1405–1413. [[CrossRef](#)]
7. Ahmadkhaniha, D.; Eriksson, F.; Leisner, P.; Zanella, C. Effect of SiC particle size and heat-treatment on microhardness and corrosion resistance of NiP electrodeposited coatings. *J. Alloy. Compd.* **2018**, *769*, 1080–1087. [[CrossRef](#)]
8. Mirak, A.; Akbari, M. Microstructural characterization of electrodeposited and heat treated Ni–B coatings. *Surf. Coat. Technol.* **2018**, *349*, 442–451. [[CrossRef](#)]
9. Bekish, Y.N.; Poznyak, S.K.; Tsybul'skaya, L.S.; Gaevskaya, T.V. Electrodeposited Ni–B alloy coatings: Structure, corrosion resistance and mechanical properties. *Electrochim. Acta* **2010**, *55*, 2223–2231. [[CrossRef](#)]
10. Kim, D.; Kim, M.J.; Kim, J.S.; Kim, H.P. Material characteristics of Ni–P–B electrodeposits obtained from a sulfamate solution. *Surf. Coat. Technol.* **2008**, *202*, 2519–2526. [[CrossRef](#)]
11. Ünal, E.; Yaşar, A.; Karahan, İ.H. A review of electrodeposited composite coatings with Ni–B alloy matrix. *Mater. Research Exp.* **2019**, *6*, 1–18. [[CrossRef](#)]
12. Torabinejad, V.; Rouhaghdam, A.S.; Aliofkhaezraei, M.; Allahyarzadeh, M.H. Ni–Fe–Al<sub>2</sub>O<sub>3</sub> electrodeposited nanocomposite coating with functionally graded microstructure. *Bull. Mater. Sci.* **2016**, *39*, 857–864. [[CrossRef](#)]
13. Garcia, I.; Fransaeer, J.; Celis, J.P. Electrodeposition and sliding wear resistance of nickel composite coatings containing micron and submicron SiC particles. *Surf. Coat. Technol.* **2001**, *148*, 171–178. [[CrossRef](#)]
14. Zanella, C.; Lekka, M.; Bonora, P.L. Influence of the particle size on the mechanical and electrochemical behaviour of micro- and nano-nickel matrix composite coatings. *J. Appl. Electrochem.* **2009**, *39*, 31–38. [[CrossRef](#)]
15. Papavasiliopoulou, P.; Pavlatou, E.; Spyrellis, N. Effect of plating parameters on NiP–SiC electrodeposition. In Proceedings of the 7th International Conference—The Coatings in Manufacturing Engineering, Kallithea, Greece, 1–3 October 2008; pp. 417–425.
16. Gül, H.; Kılıç, F.; Uysal, M.; Aslan, S.; Alp, A.; Akbulut, H. Effect of particle concentration on the structure and tribological properties of submicron particle SiC reinforced Ni metal matrix composite (MMC) coatings produced by electrodeposition. *Appl. Surf. Sci.* **2012**, *258*, 4260–4267. [[CrossRef](#)]
17. Sheu, H.H.; Huang, P.C.; Tsai, L.C.; Hou, K.H. Effects of plating parameters on the Ni–P–Al<sub>2</sub>O<sub>3</sub> composite coatings prepared by pulse and direct current plating. *Surf. Coat. Technol.* **2013**, *235*, 529–535. [[CrossRef](#)]

18. Thiemig, D.; Bund, A.; Talbot, J.B. Influence of hydrodynamics and pulse plating parameters on the electrocodeposition of nickel-alumina nanocomposite films. *Electrochim. Acta* **2009**, *54*, 2491–2498. [[CrossRef](#)]
19. Alirezaei, S.; Monirvaghefi, S.M.; Salehi, M.; Saatchi, A.; Kargosha, M. Effect of alumina content on wear behaviour of Ni–P–Al<sub>2</sub>O<sub>3</sub>( $\alpha$ ). *Surf. Eng.* **2005**, *21*, 60–66. [[CrossRef](#)]
20. Malfatti, C.F.; Veit, H.M.; Menezes, T.L.; Ferreira, J.Z.; Rodriguês, J.S.; Bonino, J. The surfactant addition effect in the elaboration of electrodeposited NiP–SiC composite coatings. *Surf. Coat. Technol.* **2007**, *201*, 6318–6324. [[CrossRef](#)]
21. Chen, L.; Wang, L.; Zeng, Z.; Zhang, J. Effect of surfactant on the electrodeposition and wear resistance of Ni–Al<sub>2</sub>O<sub>3</sub> composite coatings. *Mater. Sci. Eng. A* **2006**, *434*, 319–325. [[CrossRef](#)]
22. Rezaei-Sameti, M.; Nadali, S.; Falahatpisheh, A.; Rakhshi, M. The effects of sodium dodecyl sulfate and sodium saccharin on morphology, hardness and wear behavior of Cr–WC nano composite coatings. *Solid State Commun.* **2013**, *159*, 18–21. [[CrossRef](#)]
23. Ünal, E.; Karahan, İ.H. Effects of ultrasonic agitation prior to deposition and additives in the bath on electrodeposited Ni–B/hBN composite coatings. *J. Alloy. Compd.* **2018**, *763*, 329–341. [[CrossRef](#)]
24. Beltowska-Lehman, E.; Indyka, P.; Bigos, A.; Szczerba, M.J.; Kot, M. Ni–W/ZrO<sub>2</sub> nanocomposites obtained by ultrasonic DC electrodeposition. *Mater. Des.* **2015**, *80*, 1–11. [[CrossRef](#)]
25. Walsh, F.C.; Low, C.T.J.; Bello, J.O. Influence of surfactants on electrodeposition of a Ni-nanoparticulate SiC composite coating. *Int. J. Surf. Eng. Coat.* **2015**, 2967. [[CrossRef](#)]
26. Gül, H.; Kilic, F.; Aslan, S.; Alp, A.; Akbulut, H. Characteristics of electro-co-deposited Ni–Al<sub>2</sub>O<sub>3</sub> nano-particle reinforced metal matrix composite (MMC) coatings. *Wear* **2009**, *267*, 976–990. [[CrossRef](#)]
27. Bakhit, B.; Akbari, A. A comparative study of the effects of saccharin and  $\beta$ -SiC nano-particles on the properties of Ni and Ni–Co alloy coatings. *Surf. Coat. Technol.* **2014**, *253*, 76–82. [[CrossRef](#)]
28. Chen, F.J.; Pan, Y.N.; Lee, C.Y.; Lin, C.S. Internal stress control of Nickel-Phosphorus electrodeposits using Pulse currents. *J. Electrochem. Soc.* **2010**, *157*, D154. [[CrossRef](#)]
29. Hansal, W.E.G.; Sandulache, G.; Mann, R.; Leisner, P. Pulse-electrodeposited NiP–SiC composite coatings. *Electrochim. Acta* **2013**, *114*, 851–858. [[CrossRef](#)]
30. Berkh, O.; Bodnevas, A.; Zahavi, J. Electrodeposited Ni–P–SiC composite coatings. *Plat. Surf. Finish.* **1995**, *82*, 62–66.
31. Tamilarasan, T.R.; Rajendran, R.; Rajagopal, G.; Sudagar, J. Effect of surfactants on the coating properties and corrosion behaviour of Ni–P-nano-TiO<sub>2</sub> coatings. *Surf. Coat. Technol.* **2015**, *276*, 320–326. [[CrossRef](#)]
32. Sen, R.; Bhattacharya, S.; Das, S.; Das, K. Effect of surfactant on the co-electrodeposition of the nano-sized ceria particle in the nickel matrix. *J. Alloy. Compd.* **2010**, *489*, 650–658. [[CrossRef](#)]
33. Benea, L.; Bonora, L.; Borello, A.; Martelli, S. Composite electrodeposition to obtain nanostructured coatings. *J. Elec. Soc.* **2001**, *148*, 461–465. [[CrossRef](#)]
34. Rudnik, E.; Burzy, L.; Dolasi, Ł.; Misiak, M. Electrodeposition of nickel/SiC composites in the presence of cetyltrimethylammonium bromide. *Appl. Surf. Sci.* **2010**, *256*, 7414–7420. [[CrossRef](#)]
35. Kan, H.; Feng, X.; Wei, X.; Zhang, N.; Wang, X.; Long, H. Effects of surfactants SDS and CTAB on Ni–SiC deposition. *J. Wuhan Univ. Technol. Mater. Sci.* **1901**, *33*, 836–842. [[CrossRef](#)]
36. Hou, K.H.; Ger, M.D.; Wang, L.M.; Ke, S.T. The wear behaviour of electro-codeposited Ni–SiC composites. *Wear* **2002**, *253*, 994–1003. [[CrossRef](#)]
37. Vaezi, M.R.; Sadrnezhaad, S.K.; Nikzad, L. Electrodeposition of Ni–SiC nano-composite coatings and evaluation of wear and corrosion resistance and electroplating characteristics. *Colloids Surf. A Physicochem. Eng. Asp.* **2008**, *315*, 176–182. [[CrossRef](#)]
38. Spyrells, N.; Pavlatou, E.A.; Spanou, S.; Zoikis-Karathansis, A. Nickel and nickel-phosphorous matrix composite electrocoatings. *Trans. Nonferrous Met. Soc. China* **2009**, *19*, 800–804. [[CrossRef](#)]
39. Chou, M.C.; Der Ger, M.; Ke, S.T.; Huang, Y.R.; Wu, S.T. The Ni–P–SiC composite produced by electro-codeposition. *Mater. Chem. Phys.* **2005**, *92*, 146–151. [[CrossRef](#)]
40. Sarret, M.; Müller, C.; Amell, A. Electroless NiP micro- and nano-composite coatings. *Surf. Coat. Technol.* **2006**, *201*, 389–395. [[CrossRef](#)]
41. Mafi, I.R.; Dehghanian, C. Comparison of the coating properties and corrosion rates in electroless Ni–P/PTFE composites prepared by different types of surfactants. *Appl. Surf. Sci.* **2011**, *257*, 8653–8658. [[CrossRef](#)]

42. Sudagar, J.; Lian, J.S.; Jiang, Q.; Jiang, Z.H.; Li, G.Y.; Elansezhian, R. The performance of surfactant on the surface characteristics of electroless nickel coating on magnesium alloy. *Prog. Org. Coat.* **2012**, *74*, 788–793. [[CrossRef](#)]
43. Grosjean, A.; Rezrazi, M.U.; Berc, P. Some morphological characteristics of the incorporation of silicon carbide SiC/particles into electroless nickel deposits. *Surf. Coat. Technol.* **2000**, *130*, 252–256. [[CrossRef](#)]
44. Kalantary, M.R.; Holbrook, K.A.; Wells, P.B. Optimisation of a bath for electroless plating and its use for the production of nickel-phosphorus-silicon carbide coatings. *Int. J. Surf. Eng. Coat.* **2017**, 55–61. [[CrossRef](#)]
45. Amell, A.; Muller, C.; Sarret, M. Influence of fluorosurfactants on the codeposition of ceramic nanoparticles and the morphology of electroless NiP coatings. *Surf. Coat. Technol.* **2010**, *205*, 356–362. [[CrossRef](#)]
46. Sohrabi, A.; Dolati, A.; Ghorbani, M.; Monfared, A.; Stroeve, P. Nanomechanical properties of functionally graded composite coatings: Electrodeposited nickel dispersions containing silicon micro- and nanoparticles. *Mater. Chem. Phys.* **2010**, *121*, 497–505. [[CrossRef](#)]
47. Ger, M. Electrochemical deposition of nickel/SiC composites in the presence of surfactants. *Mater. Chem. Phys.* **2004**, *87*, 67–74. [[CrossRef](#)]
48. Alexis, J.; Etcheverry, B.; Beguin, J.D.; Bonino, J.P. Structure, morphology and mechanical properties of electrodeposited composite coatings Ni-P/SiC. *Mater. Chem. Phys.* **2010**, *120*, 244–250. [[CrossRef](#)]



© 2019 by the authors. Licensee MDPI, Basel, Switzerland. This article is an open access article distributed under the terms and conditions of the Creative Commons Attribution (CC BY) license (<http://creativecommons.org/licenses/by/4.0/>).